JOURNAL OF MATERIALS SCIENCE 24 (1989) 2239–2244

Comparative study of the surface oxidation behaviour of amorphous and crystallized $Fe_{67}Co_{18}B_{14}Si_1$ metallic glass

D. J. DE WET*, G. N. VAN WYK
Department of Physics, University of the Orange Free State, PO Box 339 Bloemfontein, 9300, Republic of South Africa

The oxidation of amorphous and crystallized specimens of the metallic glass $Fe_{67}Co_{18}B_{14}Si_1$ were studied under controlled conditions using Auger electron spectroscopy and X-ray photoelectron spectroscopy. The different oxides were characterized as boron and iron oxide forming in that sequence for both the amorphous and crystalline specimens. No cobalt oxide was detected. A higher oxygen uptake was measured for the amorphous than for the crystalline specimens. Comparison with the literature shows that the difference in oxygen uptake is heavily composition dependent. The oxidation of the amorphous specimens constitutes a driving force for boron to segregate to the surface and causes a boron enriched layer. Segregation of boron and cobalt occurs during annealing and the sequence of the enriched layers is influenced by environmental conditions.

1. Introduction

Metallic glasses are currently becoming increasingly important for industrial applications because they exhibit properties which are superior to those of their crystalline counterparts. It is, however, of great importance that these alloys should be thermally stable in the temperature ranges in which they are to be used. To explain relaxation and crystallization behaviour, diffusion data is required, which is extremely difficult to measure because of the narrow temperature range in which one can operate and the small D-values which are to be measured.

In a recent study [1] of the diffusion behaviour of silicon in metallic glasses, it was attempted [2] to conduct electron microscope studies of structural changes in metallic glasses after various heat treatments below the crystallization temperature. Difficulties were however encountered during the electrolytic thinning process. The amorphous specimens polished finely, and suitable specimens were easily obtained. The crystallized specimens however behaved quite differently in that their surfaces blackened during the thinning process. Although it was not specifically mentioned, the same problem was probably encountered by Grundy *et al.* [3] who used the electrolytic process to thin the amorphous specimens, but ion milling to thin the crystallized specimens.

To explain the above phenomenon it was decided to look at the problem in a less complicated manner and to investigate whether or not the oxidation behaviour of the crystalline and amorphous specimens differs. Surprisingly little information is available on the oxidation of metallic glasses. A few oxidation studies have been done on various iron and nickel based alloys [4–7] and to our knowledge only one investigation by Karve *et al.* [8] was done on Metglas 2605 CO, which is the glass investigated in this study. The aim of this paper is to present comparative results on the surface oxidation behaviour of the metallic glass $Fe_{67}Co_{18}B_{14}Si_1$ with that of crystallized specimens of the same composition. *In situ* oxidation were done at room temperature in ultra-high vacuum (UHV) and the analysis was done by Auger electron spectroscopy (AES) and X-ray photoelectron spectroscopy (XPS).

2. Experimental details

Metallic glass ribbons (Metglas 2605 CO) were obtained from Allied Corporation with the composition being specified as $Fe_{67}Co_{18}B_{14}Si_1$. To obtain crystalline specimens of the same composition as that of the amorphous alloy, the Metglas specimens were crystallized in a vacuum of 10^{-3} Pa with a resistance heater for 2 h at 600 $\pm$ 5° C. Temperatures were measured with a chromel–alumel thermocouple and crystallization was confirmed by X-ray diffraction measurements.

The specimens were mounted in the UHV chamber ($\simeq 10^{-9}$ torr) of a Physical Electronics Model 545 Auger/XPS system. The UHV was obtained by two adsorption roughing pumps and an ion pump assisted by a titanium sublimation pump. A 5 kV electron gun and 400 W Mg$K\alpha$ X-ray source were used for AES and XPS excitation. The energies of the Auger electrons and photoelectrons were measured with a double pass cylindrical mirror analyser (CMA) mounted coaxially with the electron gun. A 5 kV Ar^+-ion gun was used

Present address: Metals Division, National Institute for Materials Research, CSIR, PO Box 395, Pretoria 0001, South Africa.

0022–2461/89 $03.00 + .12

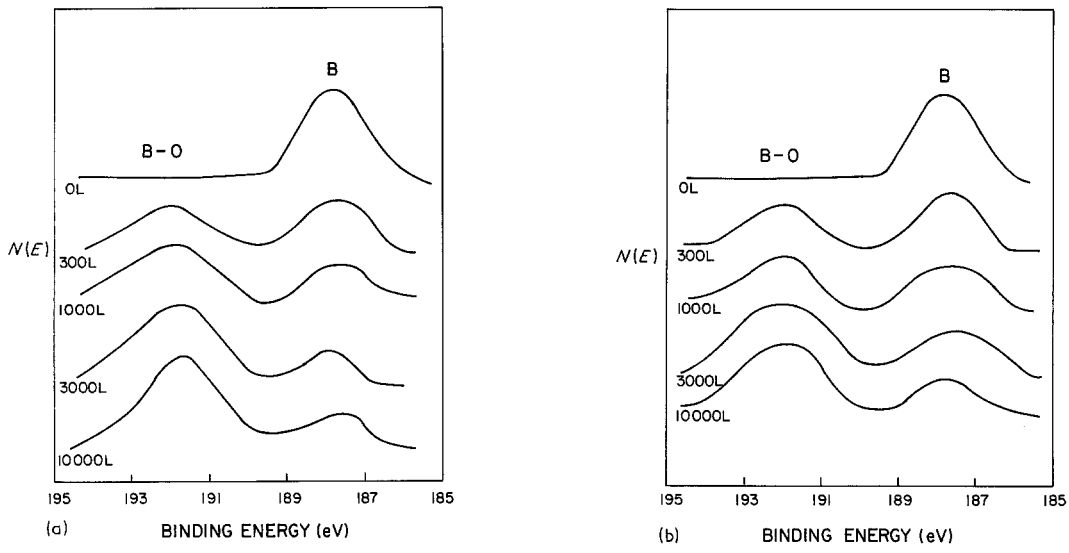

Figure 1 XPS spectra of the boron (1s) and boron oxide peaks on (a) an amorphous and (b) a crystalline specimen during controlled oxygen exposure in UHV at room temperature.

to sputter-clean the specimens prior to analysis as well as for depth profiling where the elemental distribution was recorded by a multiplexer unit during sputtering.

Controlled oxidation studies were done by exposing the specimens to different partial pressures of specpure oxygen in the UHV chamber at room temperature (25° C). Analysis of the oxide layer was done immediately under an operating vacuum of 10^{-9} torr. Before every exposure, the specimens were sputter cleaned with the Ar^+-ion gun until no oxygen peak could be detected with AES. During oxidation, the oxygen partial pressure was kept constant by slowly flowing the gas through the reaction chamber, while being monitored accurately with an Anavac residual gas analyser. The exposure was measured in langmuirs, L (1 L = 10^{-6} torr sec).

In addition the amorphous specimens were oxidized at 260° C at atmospheric pressure for 20 min by heating the specimen in air. This was done to compare the sequence in which the different oxides form with that of the oxide layer grown under controlled conditions.

Depth profiles through this oxide layer as well as an oxide layer after a 10^4 L exposure grown under controlled conditions at 25° C were done using an Ar^+-ion beam voltage of 0.5 kV and an Ar-pressure of 1.3×10^{-3} Pa. The Ar^+-ion beam was rastered maximally to enable slow enough sputtering through the oxide layers.

3. Results

3.1. XPS results

XPS spectra of the B(1s) region for the amorphous as well as the crystalline specimens are shown in Figs 1a and b, respectively, for different oxygen exposures at room temperature. Similar XPS spectra for the Fe($2p^{3/2}$) region are shown in Figs 2a and b. In order to enable a quantitative comparison between the oxidation behaviour of the crystalline and amorphous specimens, the XPS spectra for these specimens after exposures of 10^4 L and 3×10^2 L were extracted from Figs 1 and 2 and presented in Fig 3a and b.

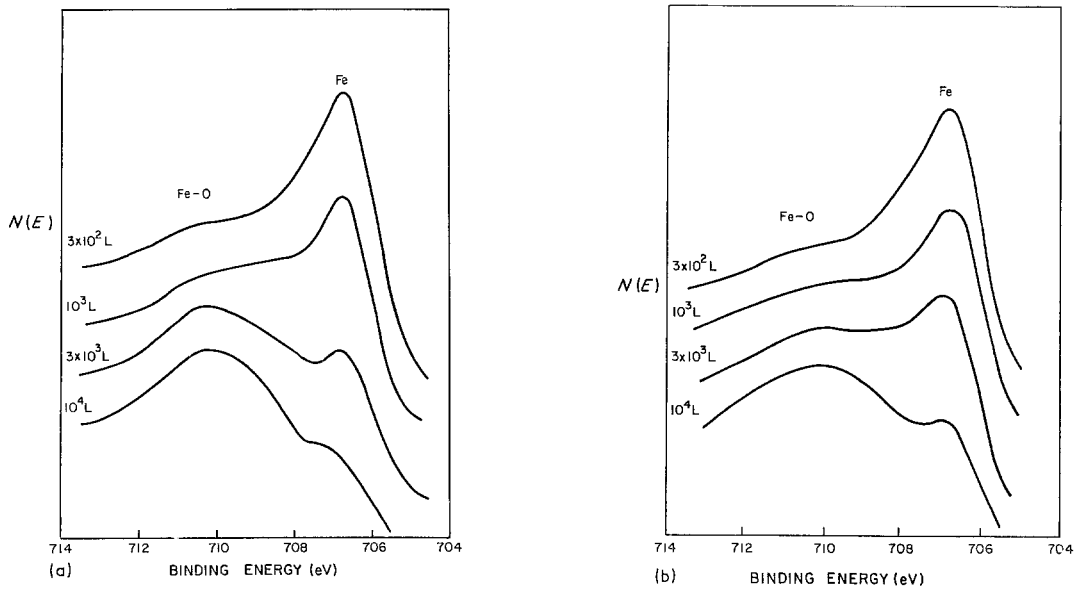

Figure 2 XPS spectra of the iron ($2p^{3/2}$) and iron oxide peaks on (a) an amorphous and (b) a crystalline specimen during controlled oxygen exposure in UHV at room temperature.

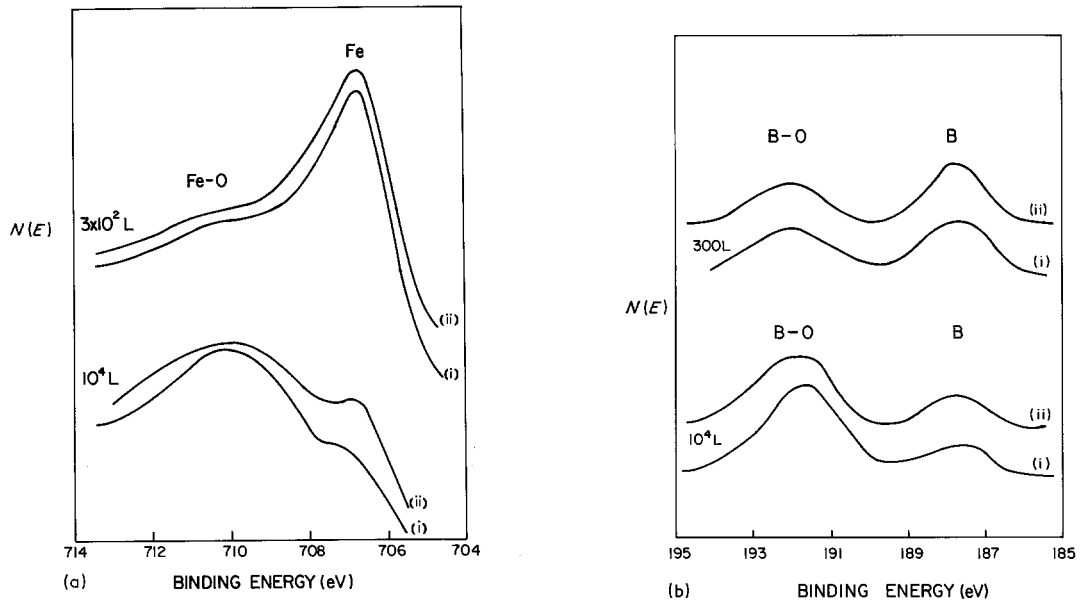

Figure 3 The comparative differences between the XPS results of (a) iron ($2p^{3/2}$) and iron oxide as well as (b) boron (1s) and boron oxide on (i) the amorphous and (ii) the crystalline specimens after controlled oxygen exposure of 300 and 10^4 L.

3.2. AES measurements and depth profiles

During AES analysis of the oxide layer it was noted that an Auger peak, additional to the normal 179 eV boron peak, appeared at 168 eV whenever boron oxide was present, as shown in Fig. 4. Boron is one of the few elements for which AES can distinguish between the pure element and the oxide [5, 8] and therefore this phenomenon is used in the quantification of the boron oxide.

Several depth profiles, as determined by AES, are presented in Figs 5–8. In Fig. 5 the concentration against depth for the different constituent elements in the as-grown amorphous alloy is shown. Fig. 6 shows the concentration profiles in the crystalline specimen, indicating a redistribution of boron and cobalt in the near surface region due to the heat treatment. The depth profile for the 10^4 L controlled oxidized specimen is shown in Fig. 7 and for the specimen oxidized in atmosphere at 260° C in Fig. 8.

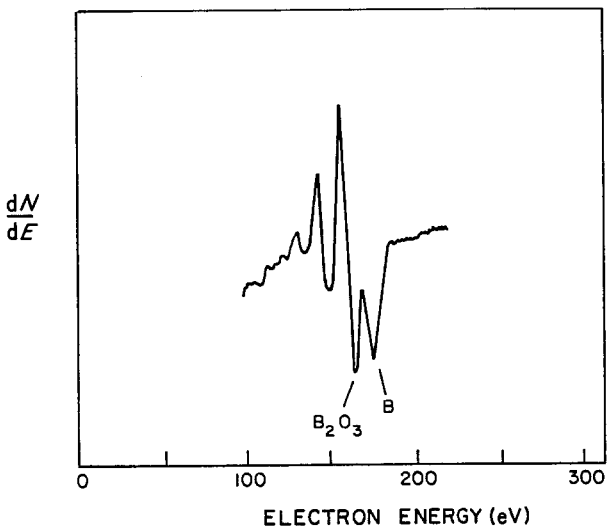

Figure 4 Part of an Auger spectrum showing the difference between boron and boron oxide (B_2O_3). The boron peak is recorded at an electron energy of 179 eV and the boron oxide peak at 168 eV.

3.3. Quantitative representation of element/oxide ratios and surface concentration

The following quantitative data was derived from the XPS and AES spectra. In Figs 9a and b the relative O : Fe and O : B ratios are presented as a function of oxygen exposure. In Figs 10a and b the same data are shown for the Fe : Fe-oxide and B : B-oxide ratios. In the case of boron use was made of the characteristic AES boron peak and in the case of iron the XPS data were used.

4. Discussion

The main features which emerge from the results are (1) the formation sequence of the oxide layers, (2) a quantitative comparison of oxidation rate between the crystalline and amorphous specimens and (3) the elemental distribution in the specimens due to oxidation or annealing. These will be discussed in the following paragraphs.

From the depth profile in Fig. 7 as well as the XPS results in Figs 1 and 2 it can be seen that boron is initially the dominant element to oxidize with a small indication of iron oxide already present at 300 L. The boron oxide is identified as B_2O_3 and the iron oxide a mixture of Fe_3O_4 and Fe_2O_3 with Fe_3O_4 probably the most dominant one [6]. The boron enrichment near the surface (Fig. 7) indicates the existence of a boron oxide layer. The depletion of boron in the bulk suggests that the surface oxidation of boron constitutes a driving force for boron to diffuse to the surface. However, the boron enrichment does not persist up to the surface. After a long enough oxygen exposure (in this case 10^4 L) the boron concentration decreases while the oxygen concentration still increases up to the surface (Fig. 7) indicating the presence of another oxide which is iron oxide according to the XPS results. No cobalt oxide was detected.

Karve *et al.* [8] also observed the segregation of boron to the surface and concluded that the oxidation of boron prevents further corrosion of the metallic

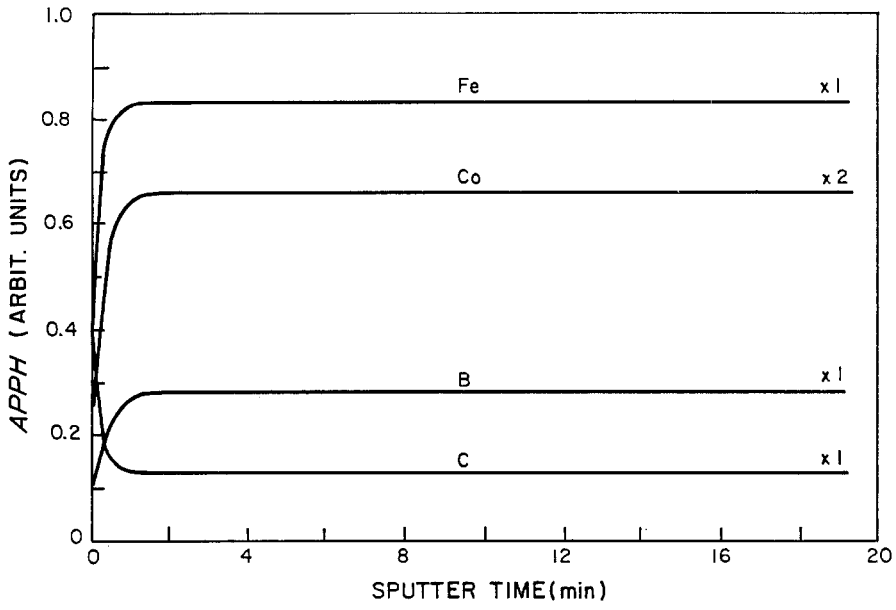

Figure 5 Depth profile of the as-prepared amorphous specimen showing the elemental distribution near the surface region. A static Ar^+-beam (3 kV, 25 mA) was used.

elements. In the study presented here the oxidation of iron was not prevented by the formation of the boron oxide layer. The above conclusions are further substantiated by the depth profile results (Fig. 8) of the thicker oxide layer formed in atmosphere at 260° C. (The sputter time cannot be compared with that in Fig. 7 because of differences in ion beam rastering.) Again a boron enrichment is observed with a subsequent cobalt enrichment. The latter will be discussed under the section elemental distribution.

The oxidation behaviour of the crystalline and amorphous specimens as discussed above was similar, the only difference being a quantitative one. From the XPS spectra (Fig. 3) as well as the AES data (Figs 9 and 10) it is evident that the amorphous specimen oxidizes at a somewhat higher rate than that of the crystallized specimen of the same composition. This is a distinguishing feature in relation to the results in the literature because the amorphous uptake is usually higher on the crystalline specimens than on the amorphous ones. For example, in the case of $Fe_{40}Ni_{38}Mo_{40}B_{18}$ [4] the crystallized and amorphous specimens behaved alike up to 100 L but at 10^4 L the oxygen uptake was 44% higher on the crystalline one. For $Ni_{76}Si_{12}B_{12}$ [4] the increase was only 13% at 10^4 L but for $Ni_{36}Fe_{32}Cr_{14}P_{12}B_6$ [7] the increase was 900% at 150 L. In this study the increase in oxygen uptake of the *amorphous* specimen above the *crystalline* one was about 8%. It is therefore clear that the difference in oxygen uptake between amorphous specimens and their crystalline counterparts is heavily composition dependent and varies over a wide range. In the case of the glass reported in this study, this difference is quantitatively not significant.

Enrichments in metallic glasses were reported in literature. Baer *et al.* [5] reported a buildup of the most noble elements below the oxide film in an amorphous FeCrNiPB specimen. Karve *et al.* [8] observed a higher cobalt content in the near surface region than in the bulk of $Fe_{67}Co_{18}B_{14}Si_2$, but no indication of the degree of cobalt enrichment is given. Schuemacher and Guiraldeno [9] annealed an amorphous FeNiPB specimen for 135 h at 150° C under an Ar-atmosphere and determined by radioactive tracer methods that phosphorus

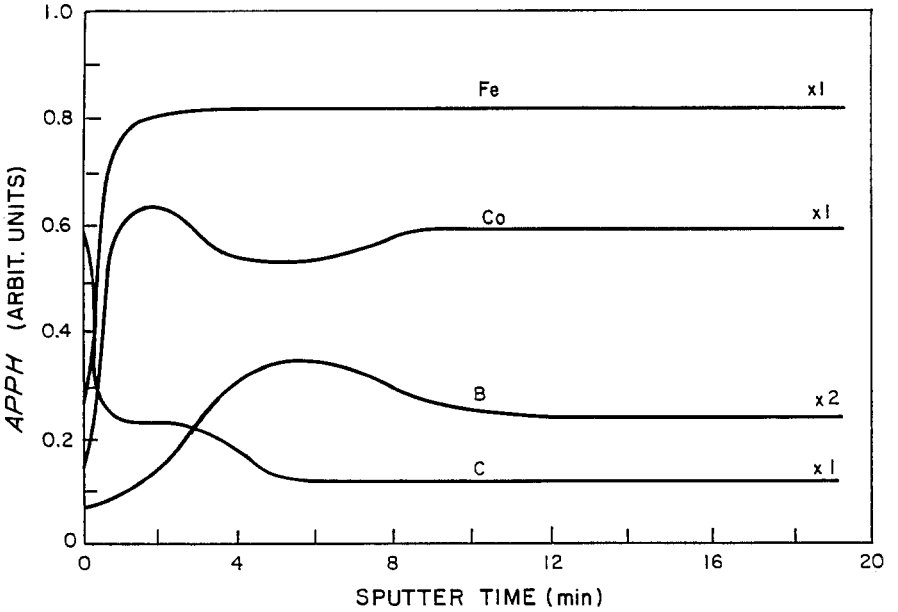

Figure 6 Depth profile of the crystallized specimen showing the elemental distribution near the surface region. The Ar^+-beam was similar to that described in Fig. 5. *APPH* = Auger Peak to Peak Heights.

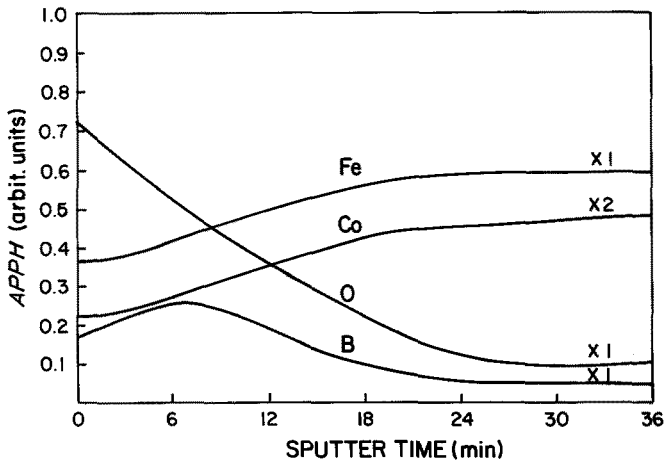

Figure 7 Depth profile through the oxide layer on an amorphous specimen after controlled oxygen exposure of 10^4 L. A rastered Ar^+-beam of 0.5 kV was used.

does not diffuse through a boron oxide layer. It is therefore of importance to discuss similar trends in this study.

All the elements were homogeneously distributed throughout the as-prepared amorphous specimen, as shown in Fig. 5. Several measurements were made and no incidental inhomogeneities were detected. The elemental distribution in the crystallized specimen is shown in Fig. 6. It is clear that segregation of cobalt and boron to the surface took place during crystallization. No carbon segregation was detected and was probably inhibited by the presence of boron. The carbon on the surface in Fig. 6 was due to contamination during annealing. The formation sequence of the segregating elements can most probably be explained by segregation theory [10, 11] but is beyond the scope of this paper. It must be noted that the enrichment of the surface by the segregating elements should not effect the oxidation behaviour because the surface was sputtered before being oxidized.

The boron enrichment in the specimen oxidized at room temperature was already discussed in the previous paragraph. In the amorphous specimen oxidized at 260° C (without being crystallized) a cobalt enrichment was found in addition to the boron enrichment which results from the tendency of cobalt to segregate to the surface. It is of importance to note that the enrichment sequence was influenced by the environmental conditions. In non-oxidizing conditions a cobalt enrichment was formed near the surface, with a boron enrichment just underneath. In oxidizing conditions the situation is reversed with additionally a hint of iron enrichment right on the surface. This situation is probably due to the fact that the surface oxidation constitutes a driving force for iron and boron to diffuse to the surface, as discussed previously.

5. Conclusions

1. Boron and iron oxide forms on both the crystallized and amorphous specimens oxidized at room temperature, with boron oxide initially the dominant one. Boron segregates during oxidation to form a boron enriched layer but after depletion of the boron, iron oxide starts to form. No cobalt oxide was detected.

2. The difference in oxidation behaviour is a quantitative one, in that a higher oxygen uptake was found on the amorphous than on the crystalline specimens.

3. A homogeneous elemental distribution was found in the as-prepared amorphous specimens, but

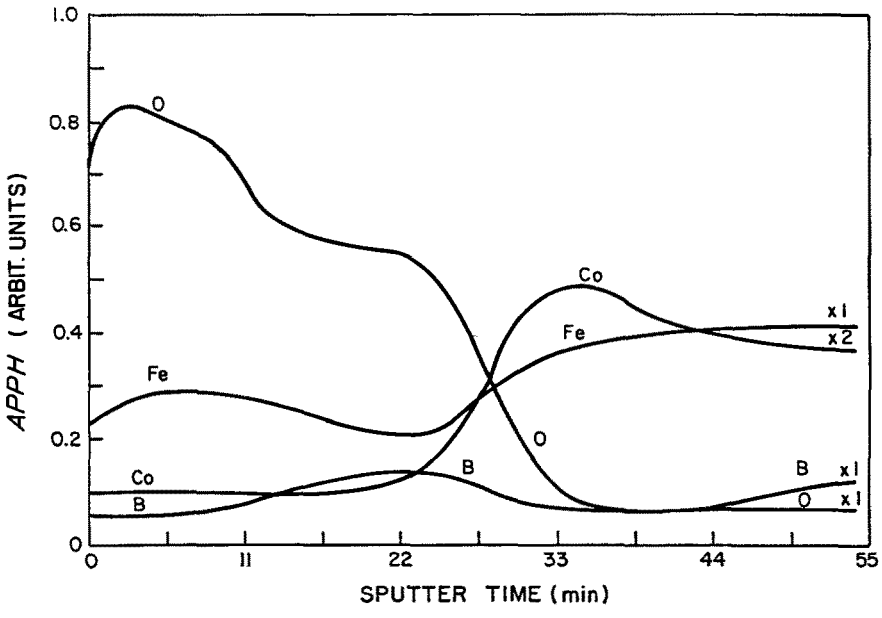

Figure 8 Depth profile through the oxide layer on an amorphous specimen after 20 min atmospheric exposure at 260° C. A rastered Ar^+-beam of 0.5 kV was used.

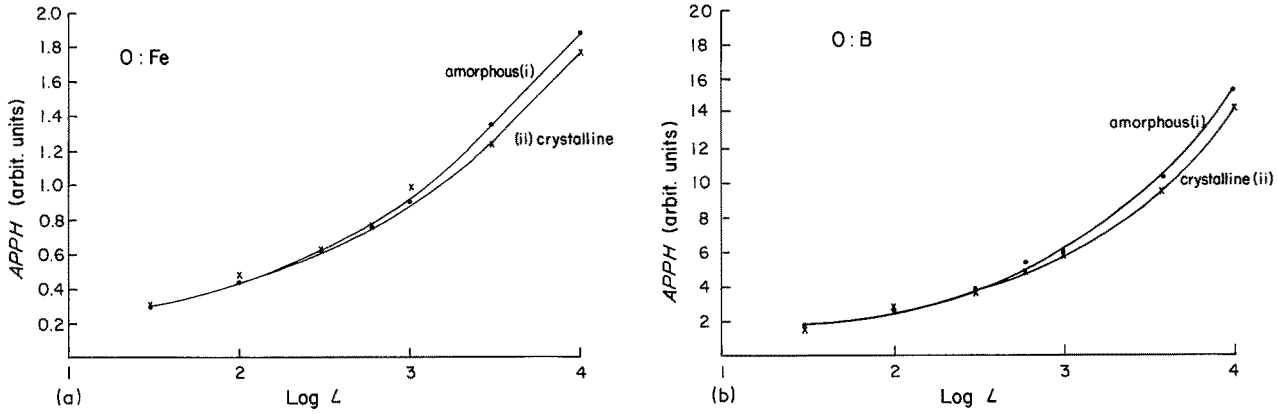

Figure 9 Oxygen uptake on (i) the amorphous and (ii) the crystalline specimens as shown by the ratios of the (a) oxygen-to-iron and (b) oxygen-to-boron Auger peak heights.

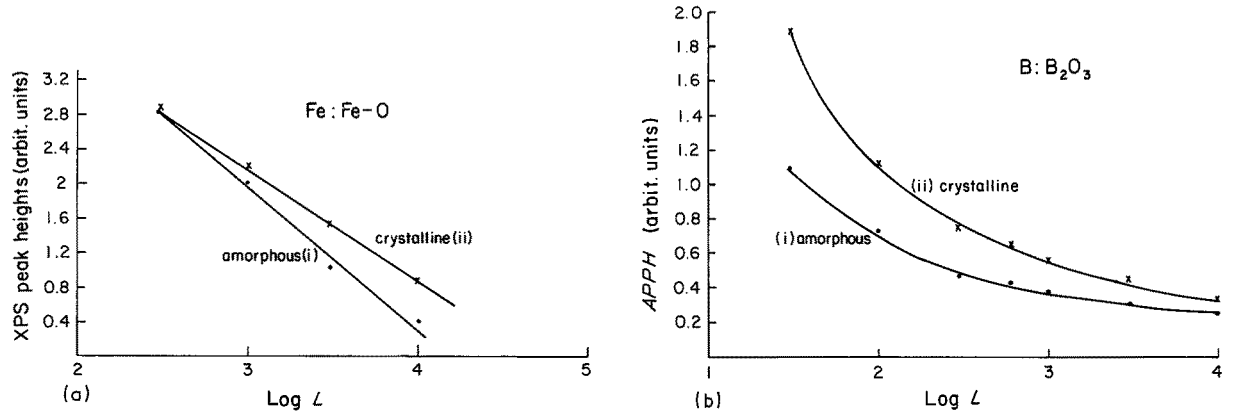

Figure 10 The ratios of XPS peak heights of (a) iron-to-iron oxide and Auger peak heights of boron-to-boron oxide for the (i) amorphous and (ii) crystalline specimens plotted against oxygen exposure.

segregation caused cobalt and boron enrichments in the crystalline specimen, with cobalt nearer to the surface.

4. During oxidation at 260° C the boron and cobalt enrichment sequence near the surface was reversed as compared to the sequence in non-oxidizing conditions because the oxidation of boron constitutes a driving force for boron to segregate to the surface.

Acknowledgements

The financial support of the Central Research Fund of this University as well as the Foundation for Research and Development is gratefully acknowledged. One of us, (DdW) would like to thank the National Institute for Materials of the CSIR for support.

References

1. G. N. VAN WYK and W. D. ROOS, *Appl. Surface Sci.* **26** (1986) 317.
2. W. D. ROOS, MSc Dissertation. University of the Orange Free State, Bloemfontein (1988).
3. P. J. GRUNDY, G. A. JONES, S. H. F. PARKER and R. S. TEBBLE, *J. Appl. Phys.* **53** (1982) 2267.
4. P. SEN, A. SRINIVASAN, M. S. HEDGE and C. N. R. RAO, *J. Mater. Sci.* **18** (1983) 173.
5. D. R. BAER, D. A. PETERSEN, L. R. PEDERSON and M. T. THOMAS, *J. Vac. Sci. Technol.* **20** (1982) 957.
6. O. HUNDERI and R. BERGERSEN, *Corros. Sci.* **22** (1982) 957.
7. P. P. KARVE, M. G. THUBE, S. K. KULKARNI and A. S. NIGAVEKAR, *Solid State Commun.* **50** (1984) 1027.
8. P. P. KARVE, S. K. KULKARNI and A. S. NIGAVEKAR, *ibid.* **49** (1984) 719.
9. J. J. SCHUEMACHER and P. GUIRALDENO, *Acta Met.* **31** (1983) 2043.
10. M. GUTTMAN and D. MACLEAN, in "Interfacial Segregation", edited by W. C. Johnson and J. M. Blakely (American Society for Metals, Cleveland, Ohio, 1977) p. 261.
11. J. DU PLESSIS and G. N. VAN WYK, *J. Phys. Chem. Solids* **49** (1988) 1441.

Received 26 January
and accepted 29 July 1988